m to 0.1 m, comparable offsets were obtained in the two regions: $\Delta z = 0.25 \pm 0.14$ m in the *Plaine des Sables* and $\Delta z = 0.31 \pm 0.29$ m in the *Enclos Fouqué*. This larger error is due to the accentuated topography and rougher surfaces. This study confirms the accuracy of the LiDAR-derived DTM that can be used to characterize small topographic features.

5.3. Normalized LiDAR intensity

LiDAR intensity, often expressed as a whole number, is the amplitude of the laser-return signal measured by the system. It depends on the peak power of the optical pulse and on the integrated energy distribution across the whole footprint (Coren & Sterzai, 2006; Höfle & Pfeifer, 2007). It is affected by atmospheric transmission, the flying altitude, the local incidence angle, surface roughness and ground reflectance (Coren & Sterzai, 2006; Höfle & Pfeifer, 2007). However it is independent of the local incidence angle, especially for low scanning angles (e.g., Mazzarini et al., 2007). Thus raw data can be used to generate a land cover classification (Maas & Vosselman, 1999). In this study, we applied a radiometric correction model based on the radar equation (Höfle & Pfeifer, 2007). It takes into account the inverse range square dependency of the received signal, the local incidence angle, and atmospheric attenuation. In clear weather, scattering and absorption of photons by gases, especially water vapor, can be neglected. Thus the simplified model giving the corrected intensity $I_{corrected}$ is expressed as:

$$I_{corrected} = I_{measured} \times \left(\frac{R}{R_s}\right)^2 \times \frac{1}{\cos(\alpha)} \quad (12)$$

with $I_{measured}$ the measured intensity, R the actual range, R_s the standard altitude and α the angle of incidence. LiDAR intensity is normalized to a standard distance of 1400 m, corresponding to the mean flying altitude, by multiplying all values by a factor of $(R/1400)^2$. This step is necessary when high elevation differences are observed. Finally, LiDAR intensity values were converted into a grid with a 1 m spatial resolution.

6. Analysis of coherence variation

6.1. Temporal decorrelation

Lava flows, pyroclastic deposits or fallen rocks cause spatial and temporal surface changes, the mapping of which is essential for understanding the evolution of the area. To evaluate the topographic changes, we compared the LiDAR data acquired in October 2008 to those acquired in November 2009. The difference between the two DTM is low, 14.9 ± 4.8 cm over the whole edifice, except over the Dolomieu crater where changes are significant. Fig. 3 shows the variations in altitude over the crater between 2008 and 2009. Negative values in dark blue point out erosion, positive values in green to red suggests deposition, and near zero values in light blue suggest no topographic changes. Such a map clearly indicates the emplacement of new lava flows in the Dolomieu crater from October 2008 to November 2009, due to the occurrence of three eruptive phases.

Fig. 4 shows the north–south and west–east topographic profiles centered in the Dolomieu crater, as well as the difference in elevation measured between 2009 and 2008. The crater floor was at an altitude of about 2200 m in 2008 and 2225 m in 2009: the area of this 25 m thick lava flow has been assessed at ~0.16 km^2 and its volume at ~2.23×10^6 m^3. This agrees with the value of $2.2 \pm 0.3 \times 10^6$ m^3 determined from the edge of the crater using a ground laser (Staudacher, 2010).

The PALSAR images acquired on September 6, 2008 and March 9, 2009 ($B_{tmp} = 184$ days, $B_{\perp} = 725$ m, $\gamma_{surface} = 0.85$) confirm the LiDAR observations. Fig. 5 shows a very low coherence over the Dolomieu crater ($\gamma = 0.38 \pm 0.11$) because of the difference in altimetry displayed in Figs. 3 and 4. Decorrelation observed over lava flows in the *Enclos Fouqué*, lapilli in the *Plaine des Sables* and vegetation in the *Grand Brûlé* and outside the caldera is basically related to the terrain type since the topographic changes are minor. This will be investigated in the next section.

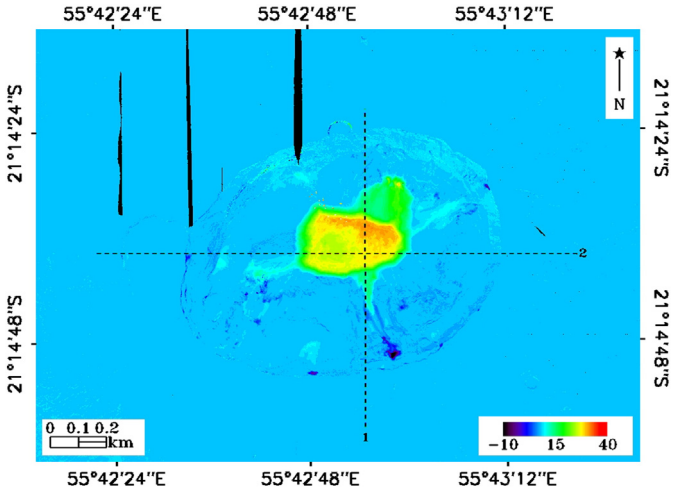

Fig. 3. Altimetry variations (in meter) between 2008 and 2009 derived from LiDAR data acquired over the Dolomieu crater. The dashed lines indicate the direction of two profiles, 1 (North–south) and 2 (West–East). (For interpretation of the references to color in this figure, the reader is referred to the web version of this article.)

6.2. Interferometric coherence vs. terrain type

Fig. 6 shows four L-band InSAR coherence maps obtained in HH polarization, with a spatial resolution of 25 m and a 46 day time interval: 3/06/08–4/21/08, 7/22/08–9/06/08, 9/06/08–10/22/08, and 7/28/10–9/12/10. Similar patterns corresponding to five distinct areas can be observed despite different baselines: the Dolomieu crater (site A), a′a lava flows in the *Enclos Fouqué* (site B), lapilli in the *Plaine des Sables* (site C), vegetation in the *Grand Brûlé* and outside the *Enclos Fouqué* (site D), and pahoehoe lava flows in the *Enclos Fouqué* (site E). Variations in coherence from one map to another may be attributed to changes in geophysical properties of the surface between two satellite tracks. The pahoehoe lava flows west of the *Enclos Fouqué* are characterized by high coherence (site E). They are made of a hard smooth crust, which is not much affected by wind or water. On the contrary, lower coherence values are observed over a′a lava flows (site B) and vegetation (site D). In the first case, it is both explained by multiple scattering from a rough surface and volume scattering in a porous material. In the second case, it is related to volume scattering and/or plant growth. In the *Plaine des Sables*, coherence degrades over lapilli (site C) owing to ground moisture variation, wind erosion or radar wave penetration into pyroclastic layers. This area is flat, reducing the topographic effects on coherence. Knowledge of the penetration depth will determine whether the radar echo is dominated by return from the surface or the subsurface.

Lu and Freymueller (1998) analyzed the SAR interferometric coherence in C-band for five typical volcanic surfaces in the Katmai volcano group, Alaska. Their results suggest that fresh lava flows have the highest coherence, followed by either weathered lava flows or fluvial deposits, and finally tephra. Lava flows maintain a good coherence since they are blocky and thus not easily modified over time unlike looser materials such as tephra. To sum up, interferometric coherence is highly spatially variable over the *Piton de la Fournaise* since it depends on surface physical properties and vegetation density. To address this issue, we will determine such variables using LiDAR and in situ ancillary data.